S©MR

СИБИРСКИЕ ЭЛЕКТРОННЫЕ
МАТЕМАТИЧЕСКИЕ ИЗВЕСТИЯ
Siberian Electronic Mathematical Reports
http://semr.math.nsc.ru
ISSN 1813-3304

Vol. 21, No. 2, pp. B64–B77 (2024)
https://doi.org/10.33048/semi.2024.21.B05

УДК 532.5
MSC 76Fxx

APPLICATION OF A TWO-DIMENSIONAL VERSION OF THE LINEARIZED GODUNOV SCHEME TO THE NUMERICAL SIMULATION OF THE KOLMOGOROV PROBLEM FOR A LIQUID POLYMER SOLUTION

V.V. DENISENKO AND **S.V. FORTOVA**

Dedicated to the memory of Sergey Godunov

Abstract: A numerical technique is proposed for modeling the flow of viscous polymer solutions and studying the phenomenon of elastic turbulence. The method is a hybridization of the numerical methods of two-dimensional linearized Godunov scheme and the Kurganov-Tadmor method. Linearized Godunov scheme was used to approximate the hydrodynamic part of the equations of a polymer solution dynamics, and is a two-dimensional method of S.K. Godunov with linear discontinuity decays, which provides guaranteed non-decreasing entropy. The flow of a Kolmogorov type polymer solution in a periodic square cell, pumped by an external periodic force and characterized by the Reynolds number $Re \sim 10^{-1}$, is investigated. The instability of the flow is obtained, the transition to the elastic turbulence regime is investigated. The spectral characteristics of the turbulent flow are constructed, and the power-law slope of the inertial interval is estimated.

Denisenko, V.V., Fortova, S.V., Application of a two-dimensional version of the linearized Godunov scheme to the numerical simulation of the Kolmogorov problem for a liquid polymer solution.

The work was performed according to state task No. 124022400174-3 "Computational experiment on supercomputers in problems of continuum mechanics".

Thanks for discussions Lebedev, V.V. and Kolokolov, I.V.

Received November, 1, 2024, Published December, 31, 2024.

Keywords: numerical modeling, elastic turbulence, hydrodynamic instability, Kolmogorov flow, numerical Godunov method.

1 Introduction

The interaction of polymer molecules with fluid flows leads to many interesting phenomena observed in nature and laboratory experiments, namely, a decrease in turbulent drag, elastic turbulence, and a change in the heat transfer process during natural convection [1, 2]. Laboratory experiments show that even a small concentration of polymers can significantly change the properties of laminar low-Reynolds ($Re \ll 1$) flows and generate a new form of turbulence called elastic (polymer) turbulence. For a Newtonian fluid flow, the transition to turbulence is determined by the nonlinear inertial term in the momentum equation or, more precisely, by the ratio of the inertial forces described by this term to the dissipative forces due to the viscosity of the medium. This ratio is characterized by a dimensionless parameter — the Reynolds number Re. The higher Re, the more unstable the flow becomes, which leads to the emergence and development of a turbulent flow regime. However, in a fluid containing polymer molecules, the so-called viscoelastic effect occurs due to the presence of another nonlinear term characterizing the influence of polymer molecules on the flow. The influence of elastic forces on the flow caused by the presence of polymers is described by another dimensionless parameter — the Weissenberg number $Wi = \frac{U}{\gamma_0 L}$ determined by the ratio of the characteristic gradient of the fluid flow velocity $\frac{U}{L}$ to the relaxation rate of the polymer molecule to its equilibrium state γ_0. As physical experiments show, the occurrence and development of flow instability at small Re occurs just because of the presence of these elastic forces [1, 2]. The flow of the polymer solution in the elastic turbulence mode is characterized by its randomness, a wide spectral range and an increase in flow resistance at fairly small values of the number $Re \ll 1$. The elastic turbulence mode is widely used in practice, for example, to mix flows characterized by small numbers $Re \ll 1$, such as flows in curved microchannels, and, accordingly, to enhance heat transfer in microchannels. Despite the huge technological interest, elastic turbulence remains poorly studied theoretically. The theoretical concepts are based on simplified viscoelastic flow models and analogies with MHD equations.

Numerical modeling of the phenomenon of elastic turbulence is a rather difficult problem. Simplified polymer models such as the Oldroyd-B model [3] and the FENE-P model [4] are mainly used to describe the polymer component. The occurrence of numerical instability is the main problem in modeling elastic turbulence using any of these models [5]. In the elastic turbulence regime, characterized by large values of the Weissenberg number $Wi > 1$, polymer molecules are quite strongly stretched, which leads to large

stress gradients in the polymer field, which are the cause of the instability of the numerical calculation.

The prerequisite for this work was the problem of developing a numerical model that could demonstrate the effects of elastic turbulence at a qualitative level. In the process of solving this problem, a two-dimensional numerical method of the second order of accuracy was constructed [6, 7], designed for direct numerical simulation of the dynamics of weakly compressible viscous flows in the presence of structural components in it. The compressible model makes it possible to apply the Godunov technique to approximate the hydrodynamic part of the defining system of equations, which makes it possible to increase the stability of the flow count in the presence of large gradients of flow parameters in them. Using this technique, the flow of a model medium at $Re \sim 10^{-1}$ is numerically studied in the presence of an external periodic force, and the instability of such a flow is obtained.

Linearized Godunov scheme, which was used in this work to approximate the hydrodynamic part of the polymer solution dynamics equations, is a method of S.K. Godunov with linear discontinuity decays, which provides guaranteed non-decreasing entropy [6, 8]. The linear simplifications introduced into the scheme are based on the use of symmetric hyperbolicity of the linearized version of the equations being solved. This hyperbolicity significantly simplifies the solution of linearized Riemann problems when finding fluxes at the boundaries of mesh cells. In addition, the calculation of each step is completed by calculating the entropy from the law of energy conservation. This scheme design ensures strict maintenance of non-decreasing entropy.

So far, we have not set the problem of obtaining results that could be used as the basis for describing real experiments on elastic turbulence. This formulation determined the choice of model relations in the development of numerical methods, as well as the selection of modeling parameters. This makes it possible to circumvent the difficulties described above that arise in numerical modeling.

2 Model equations

The equations of the polymer solution flow dynamics differ from that of a Newtonian fluid dynamics by the presence in the right part of the momentum balance equation of terms which describe the forces acting from the side of stretched polymer molecules. The proportionality coefficient A for these terms characterizes the degree of reverse influence of polymers on the flow.

Let's consider the polymer component of the flow as a structural component to the hydrodynamic flow in the form of deformable polymer molecules. The deformation is characterized by a vector $\mathbf{R}$ (R^x, R^y are its components on the OX and OY axes), which determines the direction in which the boundary of the molecular phase changes. Let's write down a system of model equations describing the dynamics of a weakly compressible viscous flow with a structural component. It consists of a system of Navier-Stokes

equations for the hydrodynamic phase of the flow and equations describing the dynamics of polymer component stretching of the flow **R** [1, 9]:

$$
\begin{aligned}
\frac{\partial \rho}{\partial t} + \nabla(\rho \mathbf{V}) &= 0,\\
\frac{\partial \rho u}{\partial t} + \nabla(\rho u \mathbf{V}) &= -\frac{\partial p}{\partial x} - \rho G \sin(ky)\cos(kx) + \mu \Delta u\\
&\quad + A\frac{\partial(\gamma(R)(R^x)^2)}{\partial x} + A\frac{\partial(\gamma(R)R^xR^y)}{\partial y},\\
\frac{\partial \rho v}{\partial t} + \nabla(\rho v \mathbf{V}) &= -\frac{\partial p}{\partial y} + \rho G \sin(kx)\cos(ky) + \mu \Delta v\\
&\quad + A\frac{\partial(\gamma(R)(R^y)^2)}{\partial y} + A\frac{\partial(\gamma(R)R^xR^y)}{\partial x},\\
\frac{\partial(\frac{\rho V^2}{2} + e)}{\partial t} &+ \nabla(\mathbf{V}(\frac{\rho V^2}{2} + e + p))\\
= \frac{\partial(\mu u \rho(\frac{\partial u}{\partial x} - \frac{\partial v}{\partial y}) + Au\gamma(R)(R^x)^2 + v\mu\rho(\frac{\partial v}{\partial x} + \frac{\partial u}{\partial y}) + Av\gamma(R)R^xR^y)}{\partial x}&\\
+ \frac{\partial(\mu u \rho(\frac{\partial u}{\partial y} + \frac{\partial v}{\partial x}) + Au\gamma(R)R^xR^y + v\mu\rho(\frac{\partial v}{\partial y} - \frac{\partial u}{\partial x}) + Av\gamma(R)(R^y)^2)}{\partial y}&\\
- u\rho G \sin(ky)\cos(kx) + v\rho G \sin(kx)\cos(ky),&\\
\frac{\partial R^x}{\partial t} + u\frac{\partial R^x}{\partial x} + v\frac{\partial R^x}{\partial y} - R^x\frac{\partial u}{\partial x} - R^y\frac{\partial u}{\partial y} + \gamma(R)R^x &= C_d \Delta R^x,\\
\frac{\partial R^y}{\partial t} + u\frac{\partial R^y}{\partial x} + v\frac{\partial R^y}{\partial y} - R^x\frac{\partial v}{\partial x} - R^y\frac{\partial v}{\partial y} + \gamma(R)R^y &= C_d \Delta R^y,\\
e = \frac{3p}{2\rho},&\\
\gamma(R) = \gamma_0(1 + \frac{R^2}{R_m^2}), \mathbf{V} = (u, v)^T.&
\end{aligned}
\tag{1}
$$

Here A is a coefficient proportional to the concentration of polymer molecules in solution which characterizes the degree of reverse influence of polymer molecules on the flow, C_d is the coefficient of polymers artificial diffusion introduced to stabilize the numerical solution, $\gamma(R)$ is the relaxation model of the polymer molecule, G is the intensity of the external force. A nonlinear approximation is used as a model of polymer elasticity $\gamma(R) = \gamma_0(1 + \frac{R^2}{R_m^2})$. Here R_m is the maximum value of stretching of the polymer molecule. Provided that $R \ll R_m$ we are dealing with a linear mode corresponding to the Oldroyd-B model [3].

The system of equations is closed using the equation of state of an ideal gas $e = \frac{3p}{2\rho}$, where the volume density of the internal energy is e [10].

The initial and boundary conditions were chosen based on considerations of the stability of the numerical experiment and the possibility of observing

the elastic turbulence regime. The values of the velocity components at the initial moment of time u, v were assumed to be zero, which corresponds to an undisturbed flow. The values of density and pressure were assumed to be equal:

$$\rho(x, y, t = 0) = 10\frac{kg}{m^3};$$
$$p(x, y, t = 0) = 10^3 Pa$$

The initial values of the components of the stretching vector of polymer molecules were:

$$R^x(x, y, t = 0) = 0.2\cos(a_x x)\, m;$$
$$R^y(x, y, t = 0) = 0.2\cos(a_y y)\, m;$$
$$a_x = 1m^{-1};$$
$$a_y = 1m^{-1}.$$

The artificial diffusion coefficient C_d was selected empirically, based on the requirements of a stable numerical calculation and the ratio $\sqrt{\frac{C_d}{\gamma_0}} \sim h$ where the characteristic cell size of the computational grid is h. The intensity of the external periodic force was assumed to be equal $G = 10^{-2}\frac{N}{kg}$, the frequency of the force was $k = 2m^{-1}$. The relaxation coefficient of the polymer molecule was assumed to be $\gamma_0 = 10^{-6}s^{-1}$ the coefficient of artificial diffusion $C_d = 10^{-9}\frac{m^2}{s}$. The value of the dynamic viscosity was equal to $\mu = 0.5Pa\,s$. The value of the parameter $A = 5 \times 10^6 \frac{kg}{m^3\, s}$. The computational domain was a square with sides $L \times L = 2\pi \times 2\pi\, m \times m$, with periodic boundary conditions set on its edges, and was covered with a uniform computational grid of 250×250 cell dimensions.

3 Numerical method

To numerically approximate the system 1, a combination of two numerical methods was used – the linearized Godunov method [6] and the Kurganov-Tadmor method [7]. The linearized Godunov method approximated the hydrodynamic part of the computational model – the Navier-Stokes system of equations, and the equations describing the polymer component of the flow were approximated by the Kurganov-Tadmor method. It should be noted that the choice of the linearized Godunov scheme for calculating the hydrodynamic part of the flow is due to the existence of large gradients of flow parameters when an elastic turbulence regime occurs. We describe a two-dimensional linearization of the Godunov method.

Let's write down the system of Navier-Stokes equations in a divergent form:

$$U_t + (F_c)_x + (G_c)_y = (F_v)_x + (F_p)_x + (G_v)_y + (G_p)_y;$$

$$U = \begin{pmatrix} \rho \\ \rho u \\ \rho v \\ \frac{\rho \mathbf{V^2}}{2} + e \end{pmatrix}; F_c = \begin{pmatrix} \rho u \\ \rho u^2 + p \\ \rho uv \\ u(\frac{\rho \mathbf{V^2}}{2} + p + e) \end{pmatrix}; G_c = \begin{pmatrix} \rho v \\ \rho uv \\ \rho v^2 + p \\ v(\frac{\rho \mathbf{V^2}}{2} + p + e) \end{pmatrix};$$

$$F_v = \mu \begin{pmatrix} 0 \\ \frac{\partial u}{\partial x} \\ \frac{\partial v}{\partial x} \\ u\rho(\frac{\partial u}{\partial x} - \frac{\partial v}{\partial y}) + v\rho(\frac{\partial v}{\partial x} + \frac{\partial u}{\partial y}) \end{pmatrix}; G_v = \mu \begin{pmatrix} 0 \\ \frac{\partial u}{\partial y} \\ \frac{\partial v}{\partial y} \\ u\rho(\frac{\partial u}{\partial y} + \frac{\partial v}{\partial x}) + v\rho(\frac{\partial v}{\partial y} - \frac{\partial u}{\partial x}) \end{pmatrix};$$

$$F_p = A\gamma(R) \begin{pmatrix} 0 \\ (R^x)^2 \\ R^x R^y \\ u(R^x)^2 + vR^x R^y \end{pmatrix}; G_p = A\gamma(R) \begin{pmatrix} 0 \\ R^x R^y \\ (R^y)^2 \\ v(R^y)^2 + uR^x R^y \end{pmatrix}.$$

Viscous F_v, G_v and "polymer"F_p, G_p fluxes through the faces of the cells of the computational grid are calculated by the usual averaging $F_{p,v_{i+\frac{1}{2},j}} = \frac{1}{2}(F_{p,v_{i,j}} + F_{p,v_{i+1,j}}), G_{p,v_{i+\frac{1}{2},j}} = \frac{1}{2}(G_{p,v_{i,j}} + G_{p,v_{i+1,j}})$. Convective flows F_c, G_c are calculated using the linearized Godunov method as follows. The subscripts x, y denote the differential operators $\frac{\partial}{\partial x}, \frac{\partial}{\partial y}$ respectively.

$$P^{n+\frac{1}{2}}_{i+\frac{1}{2},j} = \frac{\frac{p^n_{i,j}}{\rho^n_{i,j}c^n_{i,j}} + \frac{p^n_{i+1,j}}{\rho^n_{i+1,j}c^n_{i+1,j}} + u^n_{i,j} - u^n_{i+1,j}}{\frac{1}{\rho^n_{i,j}c^n_{i,j}} + \frac{1}{\rho^n_{i+1,j}c^n_{i+1,j}}};$$

$$P^{n+\frac{1}{2}}_{i,j+\frac{1}{2}} = \frac{\frac{p^n_{i,j}}{\rho^n_{i,j}c^n_{i,j}} + \frac{p^n_{i,j+1}}{\rho^n_{i,j+1}c^n_{i,j+1}} + u^n_{i,j} - u^n_{i,j+1}}{\frac{1}{\rho^n_{i,j}c^n_{i,j}} + \frac{1}{\rho^n_{i,j+1}c^n_{i,j+1}}};$$

$$U^{n+\frac{1}{2}}_{i+\frac{1}{2},j} = \frac{\rho^n_{i,j}c^n_{i,j}u^n_{i,j} + \rho^n_{i+1,j}c^n_{i+1,j}u^n_{i+1,j} + p^n_{i,j} - p^n_{i+1,j}}{\frac{1}{\rho^n_{i,j}c^n_{i,j}} + \frac{1}{\rho^n_{i+1,j}c^n_{i+1,j}}};$$

$$U^{n+\frac{1}{2}}_{i,j+\frac{1}{2}} = \begin{cases} u^n_{i,j}, V^{n+\frac{1}{2}}_{i,j+\frac{1}{2}} \geq 0 \\ u^n_{i,j+1}, V^{n+\frac{1}{2}}_{i,j+\frac{1}{2}} < 0 \end{cases};$$

$$V^{n+\frac{1}{2}}_{i+\frac{1}{2},j} = \begin{cases} v^n_{i,j}, U^{n+\frac{1}{2}}_{i+\frac{1}{2},j} \geq 0 \\ v^n_{i+1,j}, U^{n+\frac{1}{2}}_{i+\frac{1}{2},j} < 0 \end{cases};$$

$$V_{i,j+\frac{1}{2}}^{n+\frac{1}{2}} = \frac{\rho_{i,j}^n c_{i,j}^n v_{i,j}^n + \rho_{i,j+1}^n c_{i,j+1}^n v_{i,j+1}^n + p_{i,j}^n - p_{i,j+1}^n}{\frac{1}{\rho_{i,j}^n c_{i,j}^n} + \frac{1}{\rho_{i,j+1}^n c_{i,j+1}^n}};$$

$$R_{i+\frac{1}{2},j}^{n+\frac{1}{2}} = \begin{cases} \rho_{i,j}^n (1 - \frac{U_{i+\frac{1}{2},j}^{n+\frac{1}{2}} - u_{i,j}^n}{c_{i,j}^n}), U_{i+\frac{1}{2},j}^{n+\frac{1}{2}} \geq 0 \\ \rho_{i+1,j}^n (1 - \frac{u_{i+1,j}^n - U_{i+\frac{1}{2},j}^{n+\frac{1}{2}}}{c_{i+1,j}^n}), U_{i+\frac{1}{2},j}^{n+\frac{1}{2}} < 0 \end{cases};$$

$$R_{i,j+\frac{1}{2}}^{n+\frac{1}{2}} = \begin{cases} \rho_{i,j}^n (1 - \frac{V_{i,j+\frac{1}{2}}^{n+\frac{1}{2}} - v_{i,j}^n}{c_{i,j}^n}), V_{i,j+\frac{1}{2}}^{n+\frac{1}{2}} \geq 0 \\ \rho_{i,j+1}^n (1 - \frac{v_{i,j+1}^n - V_{i,j+\frac{1}{2}}^{n+\frac{1}{2}}}{c_{i,j+1}^n}), V_{i,j+\frac{1}{2}}^{n+\frac{1}{2}} < 0 \end{cases}.$$

Here P, U, V, R are the fluxes of pressure, velocity and density components, respectively. Half–integer indexes refer to fluxes on the faces of cells, integers refer to the values in the center of the cell. These formulas are a consequence of the constancy at the considered time step of Riemann invariants in cells adjacent to the boundaries $i + \frac{1}{2}, j + \frac{1}{2}$. This constancy is approximated by the equalities

$$u_{i,j}^n + \frac{p_{i,j}^n}{\rho_{i,j}^n c_{i,j}^n} = U_{i+\frac{1}{2},j}^{n+\frac{1}{2}} + \frac{P_{i+\frac{1}{2},j}^{n+\frac{1}{2}}}{\rho_{i,j}^n c_{i,j}^n}; u_{i+1,j}^n + \frac{p_{i+1,j}^n}{\rho_{i+1,j}^n c_{i+1,j}^n} = U_{i+\frac{1}{2},j}^{n+\frac{1}{2}} - \frac{P_{i+\frac{1}{2},j}^{n+\frac{1}{2}}}{\rho_{i+1,j}^n c_{i+1,j}^n};$$

$$v_{i,j}^n + \frac{p_{i,j}^n}{\rho_{i,j}^n c_{i,j}^n} = V_{i,j+\frac{1}{2}}^{n+\frac{1}{2}} + \frac{P_{i,j+\frac{1}{2}}^{n+\frac{1}{2}}}{\rho_{i,j}^n c_{i,j}^n}; v_{i,j+1}^n + \frac{p_{i,j+1}^n}{\rho_{i,j+1}^n c_{i,j+1}^n} = V_{i,j+\frac{1}{2}}^{n+\frac{1}{2}} - \frac{P_{i,j+\frac{1}{2}}^{n+\frac{1}{2}}}{\rho_{i,j+1}^n c_{i,j+1}^n}.$$

which are equivalent to the above formulas.

Next, we describe the approximation of the equations to the polymer stretching vector $\mathbf{R}$. Let's write down the equations of system 1 for the components of the polymer molecules stretching vector in a divergent form:

$$\begin{pmatrix} R^x \\ R^y \end{pmatrix}_t + \begin{pmatrix} uR^x \\ uR^y \end{pmatrix}_x - \begin{pmatrix} C_d \frac{\partial R^x}{\partial x} \\ C_d \frac{\partial R^y}{\partial x} \end{pmatrix}_x + \begin{pmatrix} vR^x \\ vR^y \end{pmatrix}_y - \begin{pmatrix} C_d \frac{\partial R^x}{\partial y} \\ C_d \frac{\partial R^y}{\partial y} \end{pmatrix}_y = \begin{pmatrix} 2R^x \frac{\partial u}{\partial x} + R^y \frac{\partial u}{\partial y} + R^x \frac{\partial v}{\partial x} - \gamma(R) R^x \\ 2R^y \frac{\partial v}{\partial y} + R^y \frac{\partial u}{\partial x} + R^x \frac{\partial v}{\partial x} - \gamma(R) R^y \end{pmatrix}$$

The essence of the Kurganov-Tadmor technique is to calculate convective fluxes on the faces of the calculated cells $\begin{pmatrix} uR^x \\ uR^y \end{pmatrix}, \begin{pmatrix} vR^x \\ vR^y \end{pmatrix}$. To approximate the remaining terms (diffusion and source), the usual averaging is used on the calculated grid cells faces. Let's denote the convective flow along the axes $x, y : F = \begin{pmatrix} uR^x \\ uR^y \end{pmatrix}, G = \begin{pmatrix} vR^x \\ vR^y \end{pmatrix}$, the vector column of unknown $R = \begin{pmatrix} R^x \\ R^y \end{pmatrix}$.

Convective flows are calculated as follows:

$$F^n_{i+\frac{1}{2},j} = \frac{F((R^+_{i+\frac{1}{2},j})^n) + F((R^-_{i-\frac{1}{2},j})^n)}{2} - \frac{(a^x_{i+\frac{1}{2},j})^n}{2}((R^+_{i+\frac{1}{2},j})^n - (R^-_{i-\frac{1}{2},j})^n);$$

$$G^n_{i,j+\frac{1}{2}} = \frac{G((R^+_{i,j+\frac{1}{2}})^n) + G((R^-_{i,j-\frac{1}{2}})^n)}{2} - \frac{(a^y_{i,j+\frac{1}{2}})^n}{2}((R^+_{i,j+\frac{1}{2}})^n - (R^-_{i,j-\frac{1}{2}})^n);$$

$$(R^\pm_{i+\frac{1}{2},j})^n = R^n_{i+1,j} \mp \frac{\Delta x}{2}(R_x)^n_{i+\frac{1}{2}\pm\frac{1}{2},j}; (R^\pm_{i,j+\frac{1}{2}})^n = R^n_{i,j+1} \mp \frac{\Delta y}{2}(R_y)^n_{i,j+\frac{1}{2}\pm\frac{1}{2}};$$

$$(a^x_{i+\frac{1}{2},j})^n = \max_\pm \frac{\partial F}{\partial R}((R^\pm_{i+\frac{1}{2},j})^n) = \left|u_{i+\frac{1}{2},j}\right|;$$

$$(a^y_{i,j+\frac{1}{2}})^n = \max_\pm \frac{\partial G}{\partial R}((R^\pm_{i,j+\frac{1}{2}})^n) = \left|v_{i,j+\frac{1}{2}}\right|;$$

$$u_{i+\frac{1}{2},j} = \frac{1}{2}(u_{i,j} + u_{i+1,j}); v_{i,j+\frac{1}{2}} = \frac{1}{2}(v_{i,j} + v_{i,j+1});$$

$$(R_x)^n_{i,j} = minmod(\theta\frac{(R_x)^n_{i,j} - (R_x)^n_{i-1,j}}{\Delta x}, \frac{(R_x)^n_{i+1,j} - (R_x)^n_{i-1,j}}{2\Delta x}, \theta\frac{(R_x)^n_{i+1,j} - (R_x)^n_{i,j}}{\Delta x});$$

$$(R_y)^n_{i,j} = minmod(\theta\frac{(R_y)^n_{i,j} - (R_y)^n_{i,j-1}}{\Delta y}, \frac{(R_y)^n_{i,j+1} - (R_x)^n_{i,j-1}}{2\Delta y}, \theta\frac{(R_y)^n_{i,j+1} - (R_y)^n_{i,j}}{\Delta y});$$

$$\theta = 1.5.$$

Here, half–integer indices refer to fluxes on the cell faces, integers refer to the values in the center of the cell, u, v are the x, y components of the flow velocity, and a is the local velocity of disturbances propagation. To limit the slopes of the reconstructed solution, a minmod limiter was used in the cell.

4 Numerical experiment results

Figure 1 shows the vorticity fields of the flow for different time points t, which allow us to trace how elastic turbulence arises and develops. The value of the Reynolds number is $Re \sim 10^{-1}$, the Weissenberg number $Wi \sim 10^3$. The flow gradually loses its laminar character and by the time $t \sim 200s$ it becomes chaotic. Figures 2-3 demonstrate flow velocity fields with current lines superimposed on them and patterns of the tensile modulus of polymer molecules $R = \sqrt{(R^x)^2 + (R^y)^2}$, respectively. In Fig. 3 it can be seen that in the chaotic mode, there are areas with large gradients of polymer molecules stretching in the flow $\frac{\partial R^i}{\partial x_i} \gg 1$, which generate chaos.

Figure 4 shows a graph of the flow kinetic energy $E = \frac{\rho \mathbf{V^2}}{2}$ dependence on time t. It can be seen that by the time $t \sim 200s$ the flow is in a statistical stationary state. The presence of a maximum on this graph means that the

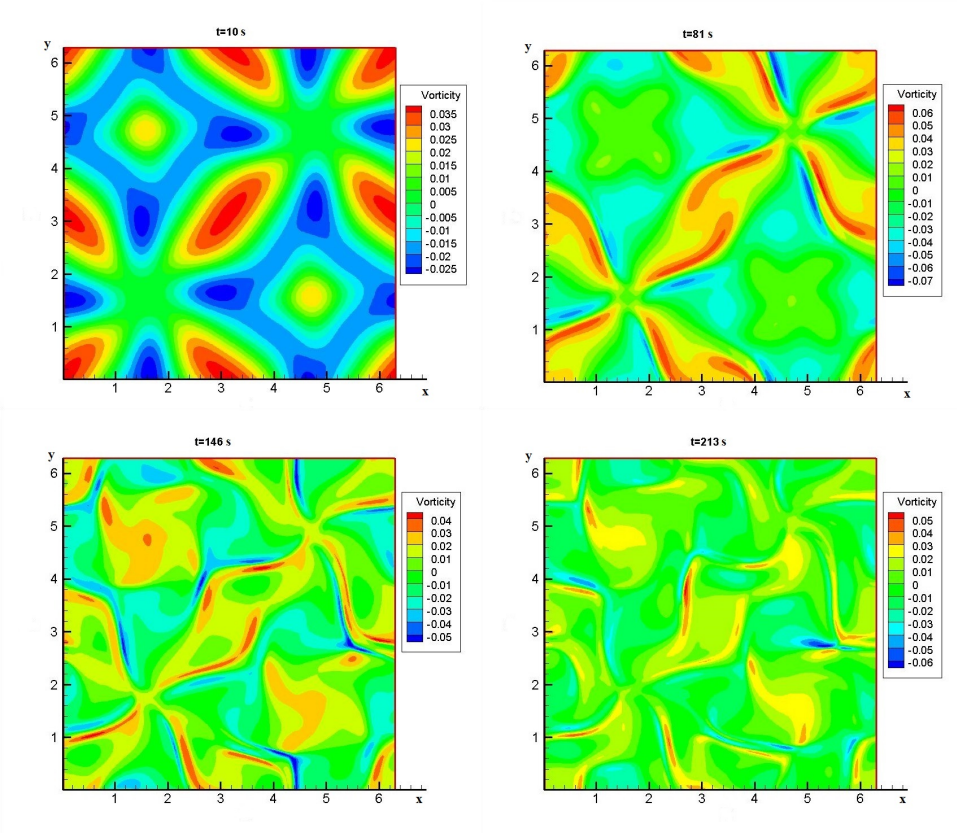

FIG. 1. The vorticity of the viscous polymer solution flow under the influence of an external periodic force in a periodic cell shows the transition to a chaotic regime.

transition to the elastic turbulence mode is accompanied by a significant transfer of the flow energy into the polymer part.

To better understand the structure of a chaotic flow, consider its spectral characteristics. Figure 5 shows the spectra of velocity E_v and stretching of polymer molecules E_r on a doubly logarithmic scale. The spectra were

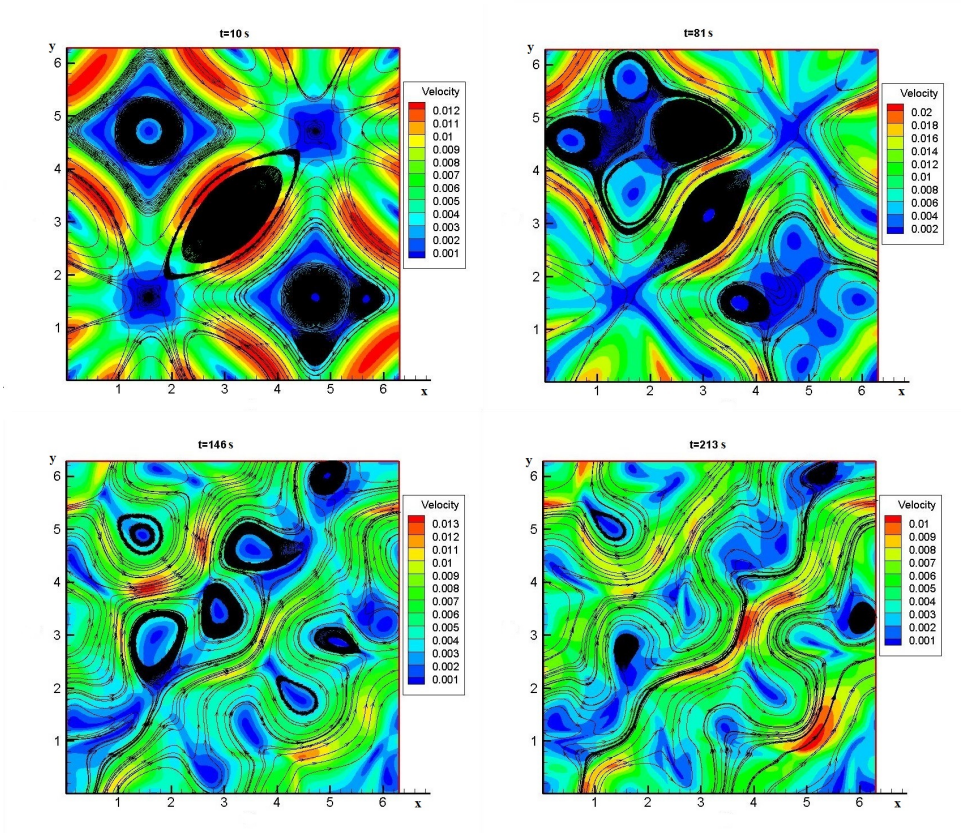

FIG. 2. Velocity fields with superimposed flow lines of a viscous polymer solution under the influence of an external periodic force in a periodic cell, a transition to a chaotic regime is shown.

calculated as a sine-cosine expansion averaged over the angles in space k_x, k_y.

$$E_v(k_x,k_y,t) = \sum_{i=0}^{1}\sum_{j=1}^{4} u^2_{i(j)}(k_x,k_y,t) +$$

$$+2\sum_{i=0}^{1}[u_{i(1)}(k_x,k_y,t)u_{i(2)}(k_x,k_y,t) + u_{i(3)}(k_x,k_y,t)u_{i(4)}(k_x,k_y,t)],$$

$$u_{i(1)}(k_x,k_y,t) = \frac{1}{\pi}\int_0^{2\pi} u_i(x,y,t)\cos(k_x x)\cos(k_y y)dxdy,$$

$$u_{i(2)}(k_x,k_y,t) = \frac{1}{\pi}\int_0^{2\pi} u_i(x,y,t)\cos(k_x x)\sin(k_y y)dxdy,$$

$$u_{i(3)}(k_x,k_y,t) = \frac{1}{\pi}\int_0^{2\pi} u_i(x,y,t)\sin(k_x x)\cos(k_y y)dxdy,$$

$$u_{i(4)}(k_x,k_y,t) = \frac{1}{\pi}\int_0^{2\pi} u_i(x,y,t)\sin(k_x x)\sin(k_y y)dxdy.$$

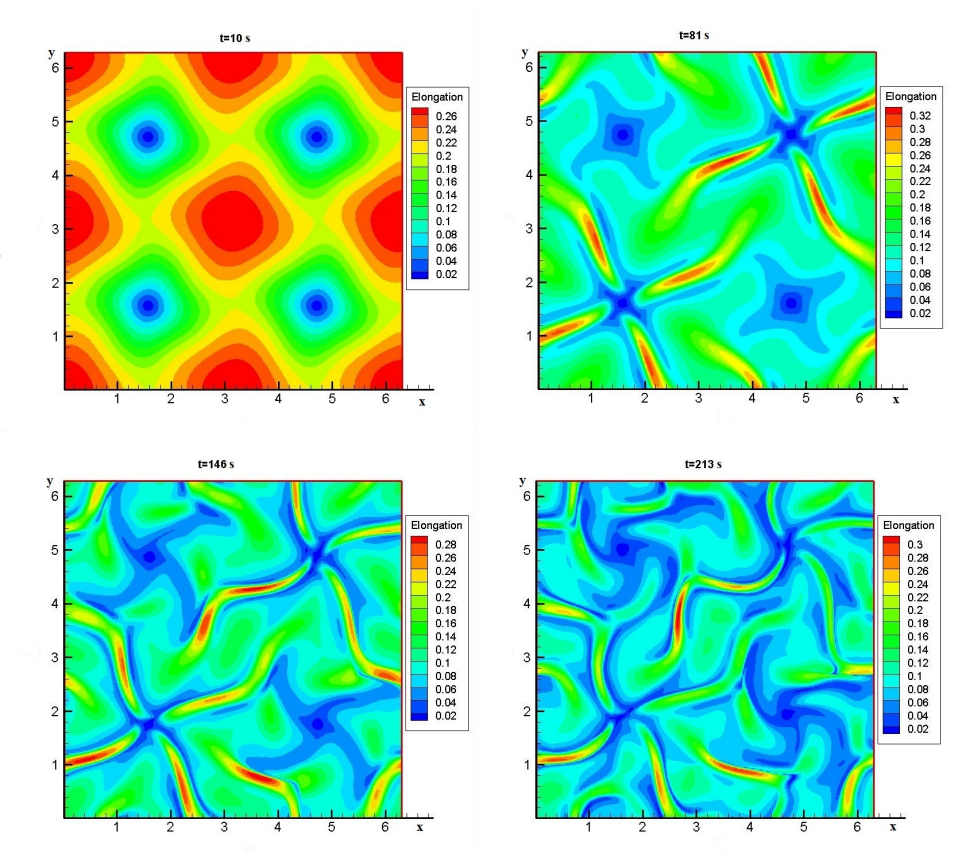

FIG. 3. The pictures of the polymer molecules stretching magnitude $R = \sqrt{(R^x)^2 + (R^y)^2}$ of the viscous polymer solution flow under the influence of an external periodic force in a periodic cell. The transition to a chaotic regime is shown.

Here the index i is entered for numbering the axial components of the velocity u, v. The wave vector $\mathbf{k}$ was averaged along the directions in the ring width $\delta = 0.5 : E(k,t) = \sum_{k_x,k_y:|k-\sqrt{k_x^2+k_y^2}|<\delta} E(k_x,k_y,t)$. The stretching spectrum $E_r(k)$ was calculated similarly by substitution $u \to R^x, v \to R^y$. Due to the chaotic nature of the flow, the spectra were additionally averaged (smoothed) also in time $E(k) = \frac{1}{T}\int_{t=t_{et}}^{t_{et}+T} E(k,t)dt, t_{et} = 200s, T = 212s$, where t_{et} denotes the time when the chaotic regime of elastic turbulence has already developed. Fig. 5 shows that the structure of the chaotic flow is such that the energy pumped by an external periodic force in the long-wave region $k_f \sim 2$ is transferred to the small-scale part of the flow (generation of a small-scale chaotic structure) through an inertial subrange characterized by a power slope ~ -3. The presence of a "shelf"in the spectra in the region

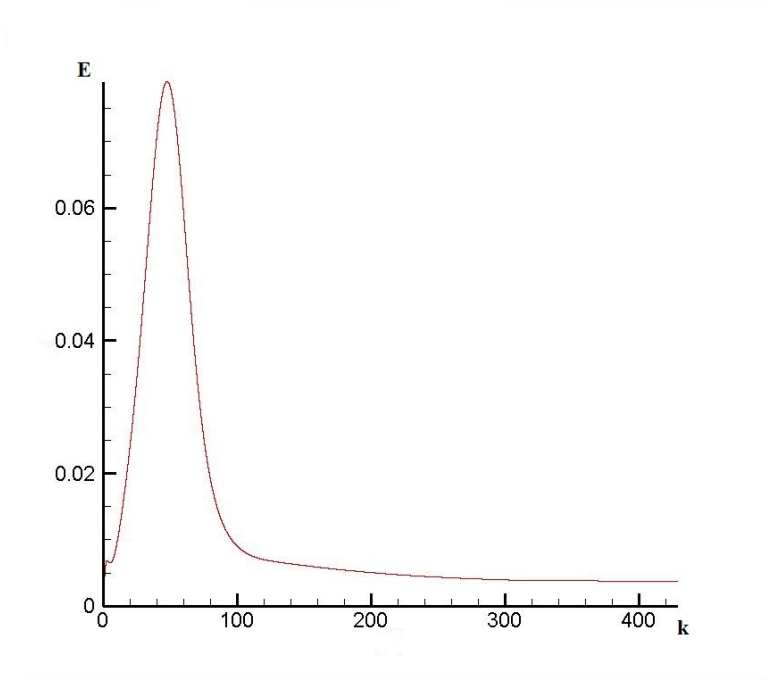

FIG. 4. Graph of the kinetic energy dependence of the flow $E = \frac{\rho \mathbf{V^2}}{2}$ on time t.

$k \sim 10^2$, which may be caused by the presence of compressibility in the system of model equations 1, requires a separate study.

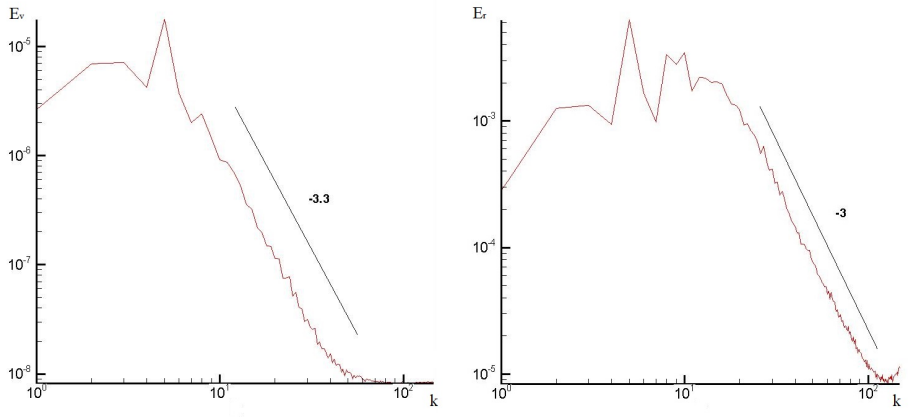

FIG. 5. Velocity spectra E_v averaged over the angles of the wave vector k and time $T = 212s$ (left) and stretching of polymer molecules E_r (right).

5 Conclusion

The paper describes a hybrid numerical method of the Godunov type, designed to approximate the model equations of the flow of a weakly compressible viscous polymer solution. The model qualitatively demonstrates the emergence and development of an elastic turbulence regime – a chaotic flow of a medium containing a polymer component. Using the example of the flow of a viscous weakly compressible polymer solution in a periodic square cell pumped by an external force, a flow with a low Reynolds number $Re \sim 10^{-1}$ and a high Weissenberg number $Wi \sim 10^3$ is studied. Using the developed numerical technique, model parameters and initial conditions under which elastic turbulence occurs were selected. Elastic instabilities arise from areas of strong stretching of polymer molecules, the development of instabilities of this type leads to the emergence of an elastic turbulence regime. The parameter characterizing the stability of polymer solution flows is the ratio between inertial forces characterized by the Reynolds number Re and elastic forces characterized by the Weissenberg number Wi. The smaller the inertia forces ($Re \ll 1$) and the greater the effect of elastic forces/ones on the flow ($Wi > 1$), the more unstable the flow of a viscous polymer solution [1].

The numerical technique developed to study the elastic instability of flows of viscous weakly compressible polymer solutions is a hybrid method of the second order accuracy approximating the equations of dynamics of a polymer solution 1. The hydrodynamic part of the system 1 is the Navier–Stokes equations, approximated by the two-dimensional linearized Godunov method [6], the polymer part is approximated by the Kurganov-Tadmor method [7]. The Godunov scheme makes it possible to improve the stability of the account due to the ability to perform calculations in areas of high gradients of hydrodynamic parameters.

In the spectral characteristics of the flow – the velocity spectrum E_v, there is an inertial range of the energy cascade with an indicator ~ -3.3. For the stretching spectrum of polymer molecules E_r, this indicator practically coincides with the indicator for $E_v \sim -3$.

References

[1] V. Steinberg, *Elastic turbulence: an experimental view on inertialess random flow*, in Moin, Parviz (ed.) et al., *Annual review of fluid mechanics*, **53** (2021), 27–58. Zbl 1459.76062

[2] A. Shahmardi, S. Zade, M.N. Ardekani, R.J. Poole, F. Lundell, M.E. Rosti, L. Brandt, *Turbulent duct flow with polymers*, J. Fluid Mech., (2019), **859**, 1057–1083. Zbl 1415.76023

[3] J.G. Oldroyd, *On the formulation of rheological equations of state*, Proc. R. Soc. Lond. Ser. A, **200**:1063 (1950), 523–541. Zbl 1157.76305

[4] A. Peterlin, *Streaming birefringence of soft linear macromolecules with finite chain length*, Polymer, **2** (1961), 257–264.

[5] M.A. Alves, P.J. Oliveira, & F.T. Pinho, *Numerical methods for viscoelastic fluid flows*, in Moin, Parviz (ed.) et al., *Annual review of fluid mechanics*, **53** (2021), 509–541. Zbl 1459.76084

[6] S.K. Godunov, V.V. Denisenko, D.V. Klyuchinskii, S.V. Fortova, V.V. Shepelev, *Study of entropy properties of a linearized version of Godunov's method*, Comput. Math. Math. Phys., **60**:4 (2020), 628–640. Zbl 1453.35126

[7] A. Kurganov, E. Tadmor, *New high-resolution central schemes for nonlinear conservation laws and convection-diffusion equations*, J. Comput. Phys., **160**:1 2000, 241–282. Zbl 0987.65085

[8] S.K. Godunov, D.V. Klyuchinskii, S.V. Fortova, V.V. Shepelev, *Experimental studies of difference gas dynamics models with shock waves*, Comput. Math. Math. Phys., **58**:8 (2018), 1201–1216. Zbl 1412.76082

[9] V.V. Denisenko, S.V. Fortova, *Numerical simulation of elastic turbulence in a confined two-dimensional cell*, J. Appl. Ind. Math. **17**:1 (2023), 43–50. Zbl 7868567

[10] L.D. Landau, E.M. Lifshitz, *Theoretical physics: Vol. VI. Gydrodynamics*, 3-e izd., Nauka, Moscow, 1986. (2003, Zbl 0997.76501)

Vladimir Viktorovich Denisenko
Institute for Computer Aided Design of the Russian Academy of Sciences,
2nd Brestskaya st., 19/18,
123056, Moscow, Russia
Email address: ned13@rambler.ru

Svetlana Vladimirovna Fortova
Institute for Computer Aided Design of the Russian Academy of Sciences,
2nd Brestskaya st., 19/18,
123056, Moscow, Russia
Email address: sfortova@mail.ru